

# Kazrin, a novel periplakin-interacting protein associated with desmosomes and the keratinocyte plasma membrane

Karen R. Groot, Lisa M. Sevilla, Kazunori Nishi, Teresa DiColandrea, and Fiona M. Watt

Keratinocyte Laboratory, Cancer Research UK London Research Institute, London WC2A 3PX, England, UK

**P**eriplakin forms part of the scaffold onto which the epidermal cornified envelope is assembled. The NH<sub>2</sub>-terminal 133 amino acids mediate association with the plasma membrane and bind a novel protein, kazrin. Kazrin is highly conserved and lacks homology to any known protein. There are four alternatively spliced transcripts, encoding three proteins with different NH<sub>2</sub> termini. Kazrin is expressed in all layers of stratified squamous epithelia; it becomes membrane associated in the suprabasal layers,

coincident with up-regulation of periplakin, and is incorporated into the cornified envelope of cultured keratinocytes. Kazrin colocalizes with periplakin and desmoplakin at desmosomes and with periplakin at the interdesmosomal plasma membrane, but its subcellular distribution is independent of periplakin. On transfection, all three kazrin isoforms have similar subcellular distributions. We conclude that kazrin is a novel component of desmosomes that associates with periplakin.

## Introduction

The cornified envelope (CE), comprising a layer of insoluble, cross-linked proteins assembled at the plasma membrane of keratinocytes in the outermost epidermal layers, is indispensable for epidermal barrier function (for reviews see Kalinin et al., 2001, 2002). Two of the earliest CE precursors to be expressed during epidermal terminal differentiation are envoplakin and periplakin, which localize to desmosomes and the interdesmosomal plasma membrane (Ruhrberg et al., 1996, 1997; DiColandrea et al., 2000). Transglutaminase 1 catalyses isopeptide bonds between envoplakin, periplakin, and a third CE precursor, involucrin, resulting in the formation of a scaffold to which other precursors are added to form the mature CE (Kalinin et al., 2001).

Envoplakin and periplakin belong to the plakin family of cytolinker proteins, whose other members include desmoplakin, plectin, and bullous pemphigoid antigen 1 (for reviews

see Fuchs and Karakesisoglou, 2001; Leung et al., 2002). Plakins link cytoskeletal networks to each other and to membrane-associated adhesive sites. The domains required for association with desmosomes and hemidesmosomes or the actin cytoskeleton are located in the NH<sub>2</sub> terminus, whereas those that bind intermediate filaments (IFs) or microtubules are found in the COOH terminus. The central coiled coil rod domain mediates homodimerization. Envoplakin and periplakin are unusual in that they can heterodimerize, and envoplakin appears to depend on periplakin both for association with the plasma membrane and for stable IF binding (Ruhrberg et al., 1997; DiColandrea et al., 2000; Karashima and Watt, 2002).

Although periplakin lacks a consensus actin-binding domain, its NH<sub>2</sub> terminus associates with cortical actin at the interdesmosomal plasma membrane, allowing it to act as a scaffold for CE assembly (DiColandrea et al., 2000). In this paper, we set out to define the mechanism by which periplakin associates with the plasma membrane.

## Results and discussion

### Defining the domains of periplakin necessary for plasma membrane localization

The 495 NH<sub>2</sub>-terminal amino acids of periplakin (P1/2N), encoding the NN, Z, Y, and X subdomains, are sufficient

Abbreviations used in this paper: CE, cornified envelope; IF, intermediate filament.

K.R. Groot, L.M. Sevilla, and K. Nishi contributed equally to this paper. The online version of this article includes supplemental material.

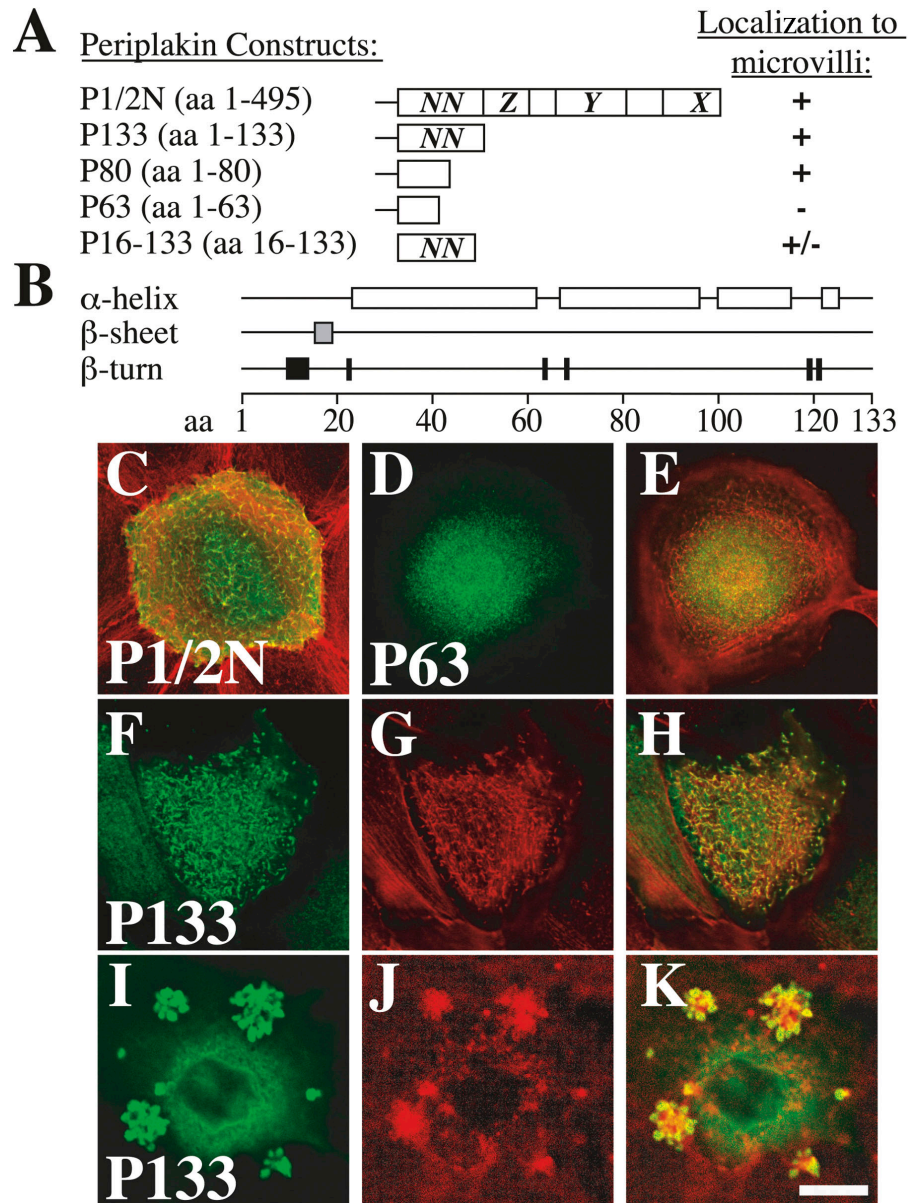
Address correspondence to F.M. Watt, Keratinocyte Laboratory, Cancer Research UK London Research Institute, 44 Lincoln's Inn Fields, London WC2A 3PX, UK. Tel.: 44 20 7269 3528. Fax: 44 20 7269 3078. email: fiona.watt@cancer.org.uk

K. Nishi's present address is Frontier Research Laboratories, Pharmaceutical Research Division, Takeda Pharmaceutical Company Ltd., 10 Wadai, Tsukuba, Ibaraki 300-4293, Japan.

T. DiColandrea's present address is Corporate Research Biotechnology, Procter and Gamble, Miami Valley Labs, Cincinnati, OH 45252.

Key words: epidermis; cornified envelope; microvilli; actin; differentiation

**Figure 1. Periplakin deletion analysis.** (A) Schematic diagram of the periplakin constructs used for transient transfections. Domain nomenclature is described by Ruhrberg et al. (1997). All constructs had COOH-terminal HA tags. (B) Secondary structure predictions based on algorithms of Chou/Fasman and Garnier/Robson of the NH<sub>2</sub>-terminal 133 amino acids of periplakin. (C–K) Confocal projections of primary keratinocytes transfected with periplakin NH<sub>2</sub>-terminal constructs (C, P1/2N; D and E, P63; F–K, P133). (I–K) Cells were treated with Latrunculin B (200 ng/ml, 3 h) before fixation. Green, anti-HA; red, phalloidin-TRITC. C, E, H, and K show merged images. Bar: (C–H) 20  $\mu$ m; (I–K) 10  $\mu$ m.



for desmosomal and interdesmosomal plasma membrane localization (DiColandrea et al., 2000). At the interdesmosomal plasma membrane, P1/2N is concentrated at microvilli, defined here as actin-rich projections from the apical surface of cultured keratinocytes (DiColandrea et al., 2000; Fig. 1 C). Further deletion constructs were generated to precisely define the membrane interaction region (Fig. 1 A). Amino acids 1–133 of periplakin (P133), encoding the entire NN subdomain and the 16 amino acids that precede it, colocalized as efficiently as P1/2N (Fig. 1 C) with cortical actin (Fig. 1, F–H) and CD44 (not depicted) at microvilli. Addition of Latrunculin B caused redistribution of both P133 and P1/2N with actin (Fig. 1, I–K; DiColandrea et al., 2000).

Sequence analysis predicts that the NN subdomain comprises four short  $\alpha$ -helices that fold into an antiparallel bundle (Fig. 1 B; Ruhrberg et al., 1997). Removal of the 16 amino acids preceding the NN subdomain prevented ef-

ficient localization to microvilli (P16-133; not depicted). When amino acids 1–63 of periplakin were expressed in keratinocytes, no specific localization to microvilli was observed (Fig. 1, D and E, P63). Amino acids 1–80 could localize to microvilli, but not in all transfectants (P80; not depicted). We conclude that P133 is the minimal region of periplakin able to localize efficiently to the plasma membrane and associate with the cortical actin cytoskeleton.

#### Identification of kazrin as a novel periplakin interactor

Because periplakin does not directly bind actin (not depicted), we performed a yeast two-hybrid screen to identify proteins that bind to the NH<sub>2</sub> terminus of periplakin and might mediate its association with actin or the plasma membrane. Using P133 as bait and a human keratinocyte cDNA library as prey, we identified a single clone. The insert DNA encoded a 279 amino acid protein in frame to the GAL4-AD domain that lacked a translation initiation codon.

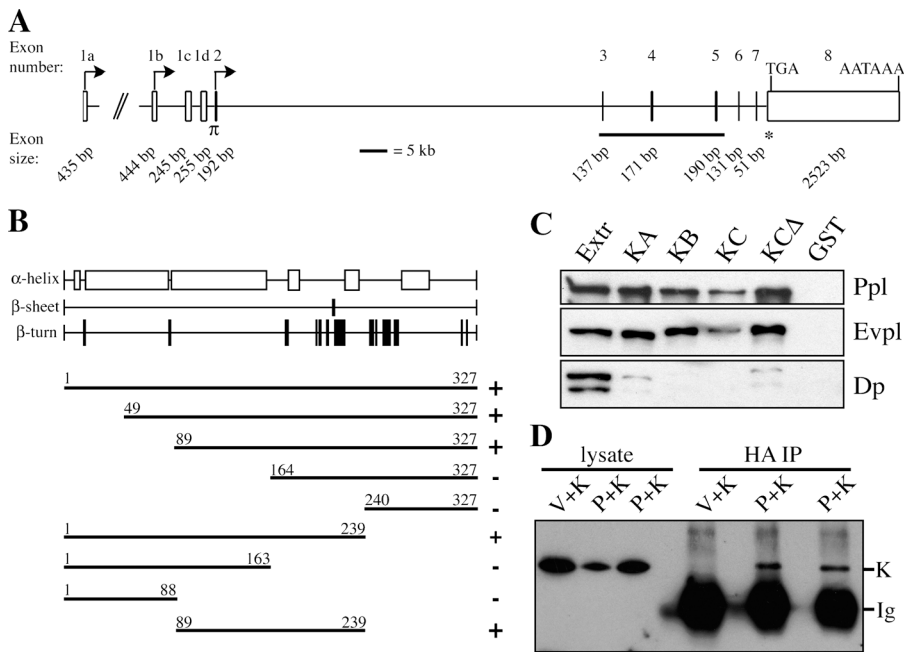


**Figure 2. Kazrin and its interaction with periplakin.** (A) Intron-exon organization of the kazrin gene, drawn to scale. Arrows, translation initiation sites; diagonal lines, 320 kb gap;  $\pi$ , leucine zipper-like domain; black bar spanning exons 3 to 5,  $\alpha$ -helical region; asterisk, putative NLS sequence. TGA, translation termination codon; AATAAA, polyadenylation signal. Sequence data available from GenBank/EMBL/DDDBJ under accession no. AY505119, AY505120, AY505121, and AY505122, corresponding to kazrin isoform a, b, c, and d, respectively. (B) Secondary structure predictions of kazrin C, based on algorithms of Chou/Fasman and Garnier/Robson, and two-hybrid analysis of interaction between P133 and kazrin deletion constructs. Numbers correspond to amino acids of kazrin C. Interactions scored positive if yeast grew on selective medium. (C) Immunoblots of GST pull-downs from keratinocyte lysates with immobilized GST-kazrin A (KA), GST-kazrin B (KB), GST-kazrin C (KC), GST-kazrin C (KCA), or GST alone (GST). Blots were probed with antibodies specific for periplakin (Ppl; TD2), envoplakin (Evpl; CR5), or desmoplakin (Dp; 115F). As a control, 4% of cell lysate used in the pull-downs was loaded on gel (Extr). (D) Coimmunoprecipitation of kazrin C with P133. Cos-7 cells were transiently transfected with kazrin C-FLAG (K) together with empty vector (V) or P133-HA (P). Proteins were immunoprecipitated with anti-HA Y11 (HA IP), and immunoblots were probed with anti-FLAG mAb M2. As a control, 5% of cell lysate used in the immunoprecipitation was run in parallel (lysate). Positions of kazrin (K) and immunoglobulin light chain (Ig) are indicated.

kazrin C aa 49–327 (KCA), or GST alone (GST). Blots were probed with antibodies specific for periplakin (Ppl; TD2), envoplakin (Evpl; CR5), or desmoplakin (Dp; 115F). As a control, 4% of cell lysate used in the pull-downs was loaded on gel (Extr). (D) Coimmunoprecipitation of kazrin C with P133. Cos-7 cells were transiently transfected with kazrin C-FLAG (K) together with empty vector (V) or P133-HA (P). Proteins were immunoprecipitated with anti-HA Y11 (HA IP), and immunoblots were probed with anti-FLAG mAb M2. As a control, 5% of cell lysate used in the immunoprecipitation was run in parallel (lysate). Positions of kazrin (K) and immunoglobulin light chain (Ig) are indicated.

A BLAST search of the nucleotide sequence of the positive clone resulted in identification of four alternatively spliced isoforms encoded by the human gene, which we have named kazrin (Fig. 2). The kazrin gene is located on human chromosome 1 (band 1p36.21) and mouse chromosome 4 (band 4E1). Each isoform of human kazrin has one of four possible first exons, referred to as 1a, 1b, 1c, or 1d (Fig. 2 A). Exons 2 to 8 are spliced together and are preceded by one of the four alternative first exons (Fig. 2 A and Fig. S1 A, available at <http://www.jcb.org/cgi/content/full/jcb.200312123/DC1>). Exons 1a and 1b contain in-frame start codons resulting in proteins of 421 (kazrin A) and 414 (kazrin B) amino acids, respectively (Fig. S1 A). The coding sequence of kazrin splice forms containing 1c or 1d begins within exon 2, resulting in a protein of 327 amino acids. Thus, kazrin C and D have identical amino acid sequences and are referred to as kazrin C for simplicity. The region of kazrin identified in the yeast two-hybrid screen corresponds to amino acids 49 to 327 of kazrin C. BLAST searches against the mouse genome revealed the presence of sequences with homology to each of the alternative first exons 1a, 1b, 1c, 1d, and exons 2–8. Thus far, however, only sequences corresponding to kazrin a and b transcripts are present in mouse EST databases.

Human kazrin is 98% identical at the protein level to the predicted amino acid sequence of mouse kazrin over the region encompassing human kazrin C. The unique protein sequences at the NH<sub>2</sub> termini of kazrin A and B are also highly conserved between mouse and human (Fig. S1 B).

All protein isoforms of kazrin are hydrophilic and lack any predicted transmembrane domain (Fig. S2, available at <http://www.jcb.org/cgi/content/full/jcb.200312123/DC1>). The

NH<sub>2</sub>-terminal portion of the protein is a highly  $\alpha$ -helical region predicted to form a coiled coil, whereas the COOH-terminal half of kazrin is predicted to contain a small  $\beta$  sheet, multiple  $\beta$ -turns, and three  $\alpha$ -helical stretches (Fig. 2 B and Fig. S2). There is weak homology between the kazrin NH<sub>2</sub>-terminal  $\alpha$ -helical region and the  $\alpha$ -helical coiled coil domain of ERM proteins (Bretscher et al., 2002). Kazrin A and B have a leucine zipper-like motif encoded by exon 2, upstream of the translation initiation codon for kazrin C (Fig. 2 A and Fig. S1 A) that could potentially mediate dimerization or interactions with other proteins. The unique NH<sub>2</sub> termini have different potential phosphorylation sites. All kazrin isoforms have a putative NLS located near the COOH terminus (Fig. 2 A and Fig. S1 A).

To map the region of kazrin responsible for periplakin binding, deletion mutants of kazrin were tested for their ability to bind P133 by yeast two-hybrid analysis (Fig. 2 B). Amino acids 89 to 239 of kazrin C, encompassing part of the  $\alpha$ -helical region and a series of  $\beta$ -turns, were sufficient to mediate the interaction with amino acids 1 to 133 of periplakin.

To validate the association of kazrin with P133, kazrin-GST fusion proteins were constructed and used in pull-down assays with human keratinocyte lysates as a source of periplakin (Fig. 2 C). The partial clone obtained in the yeast two-hybrid screen (KCA), full-length kazrin A, B, and C all bound periplakin. Envoplakin was detected in the pull-downs, suggesting that kazrin can associate with periplakin/envoplakin heterodimers. Desmoplakin was readily detected in keratinocyte lysates, but was either undetectable or weakly detectable in the pull-downs (Fig. 2 C).



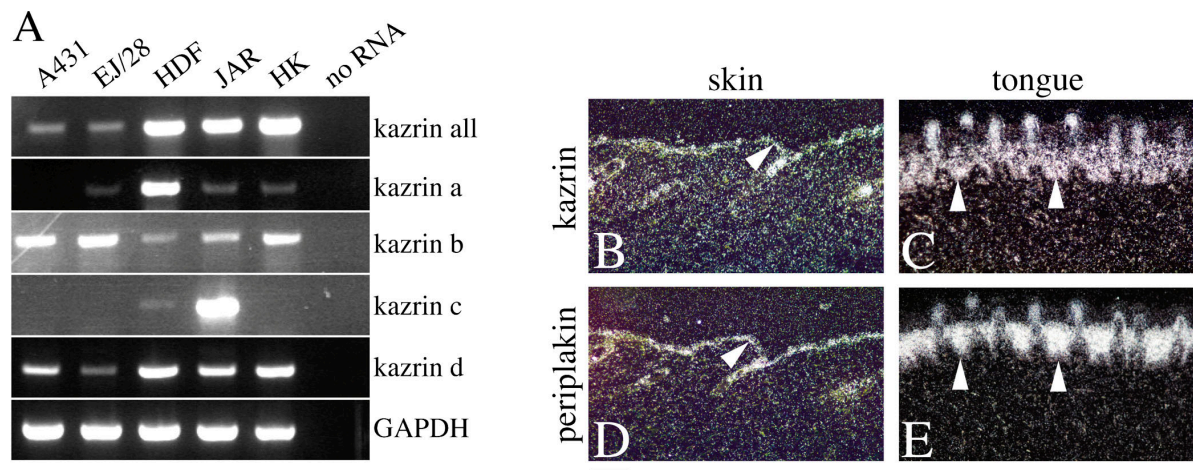


**Figure 3. Kazrin mRNA expression.** (A) RT-PCR analysis of kazrin mRNA. Forward primers specific for each of the four alternatively spliced first exons were used in combination with a reverse primer common to all splice forms. As a control for the total level of kazrin transcripts, a forward primer was used that binds within exon 2 (kazrin all) in combination with the reverse primer. Primers specific for glyceraldehyde-3-phosphate dehydrogenase (GAPDH) were used to control for input level of mRNA. (B–E) In situ hybridization of kazrin (B and C) and periplakin (D and E) using  $^{35}\text{S}$ -labeled antisense riboprobes in wild-type mouse skin (B and D) and tongue (C and E). Arrowheads show junction between epithelium and connective tissue. Bar, 100  $\mu\text{m}$ .

To examine whether or not kazrin and periplakin were capable of associating in intact cells, we cotransfected FLAG-tagged kazrin C and HA-tagged P133 into Cos-7 cells (Fig. 2 D). The transfected proteins were detected in cell lysates with the appropriate antibodies (Fig. 2 D, lysate; and not depicted). Kazrin C was coimmunoprecipitated with P133, as detected by Western blotting with anti-FLAG antibody (Fig. 2 D, HA IP).

### Expression of kazrin mRNA and alternatively spliced transcripts

Kazrin expression was analyzed by real-time PCR using cDNA preparations from multiple human tissues and cells (Fig. S3, available at <http://www.jcb.org/cgi/content/full/jcb.200312123/DC1>) and primers common to all four kazrin splice forms. Kazrin was detected in many tissues that have been demonstrated to express periplakin, including bladder, brain, colon, heart, kidney, liver, lung, pancreas, placenta, and small intestine (Ruhrberg et al., 1997; Aho and Kazerounian, 2003).

To determine if the splice variants of kazrin are differentially expressed, RT-PCR was performed on RNA isolated from primary human keratinocytes (Fig. 3 A, HK), primary dermal fibroblasts (HDF), and from three human cell lines, A431 (epidermoid carcinoma), EJ/28 (bladder carcinoma), and JAR (placental trophoblastoma). A forward primer that binds specifically within each first exon, 1a, 1b, 1c, or 1d, was used in combination with a reverse primer that binds sequences in exons 3 and 4 (Fig. 3 A). Kazrin b and d transcripts were expressed in all cell types examined. Kazrin a transcript was detectable in all cell types except A431. Kazrin c transcript was only detected in JAR cells and human dermal fibroblasts. Thus, kazrin mRNA splicing differs between cell types, and keratinocytes are predicted to express all three protein isoforms.

In situ hybridization was performed to compare kazrin and periplakin expression in mouse skin and tongue (Fig. 3, B–E),

using  $\beta$  actin as a positive control (not depicted). Periplakin and kazrin were expressed in the interfollicular epidermis and hair follicles (Fig. 3, B and D). Kazrin was also detected in the dermis (Fig. 3 B). Up-regulation of periplakin in the suprabasal layers of tongue epithelium was readily observed (Fig. 3 E). In contrast, kazrin mRNA was expressed uniformly in basal and suprabasal layers (Fig. 3 C).

### Expression and subcellular localization of kazrin protein

Affinity-purified rabbit anti-kazrin (LS4) recognized bands of  $\sim 47$  and 37 kD on Western blots of cell lysates (Fig. 4 A). These bands correspond to the predicted molecular masses of kazrin A (46.7 kD), kazrin B (46 kD), and kazrin C (37 kD). A431 cells express kazrin b but not kazrin a transcript (Fig. 3 A); nevertheless the 47-kD protein band from A431 lysates appeared as a doublet, suggesting kazrin may undergo posttranslational modification (Fig. 4 A). Although A431, EJ/28, and human keratinocytes expressed similar levels of kazrin d transcript (Fig. 3 A), the 37-kD form of kazrin protein was relatively less abundant in human keratinocytes, an indication of differential regulation at the translational or posttranslational level.

To determine whether or not kazrin, like periplakin, can be incorporated into the CE, confluent keratinocyte cultures were treated with 0.04% Triton X-100 for 5 h to induce envelope assembly (Fig. 4 B). Proteins that become cross-linked into the CE are no longer extractable in SDS and reducing agents. Transglutaminase-mediated cross-linking is inhibited by 20 mM cystamine (Ruhrberg et al., 1997). Periplakin and kazrin were readily detected in control cell lysates in the presence (Fig. 4 B, Cy) or absence (Fig. 4 B, –) of cystamine. Both proteins became nonextractable after Triton X-100 incubation (Fig. 4 B, T), and this was inhibited by cystamine (Fig. 4 B, Cy/T). We conclude that kazrin can be incorporated into the CE.

Consistent with the in situ hybridization results (Fig. 3, B and C), kazrin protein was detected in all layers of human

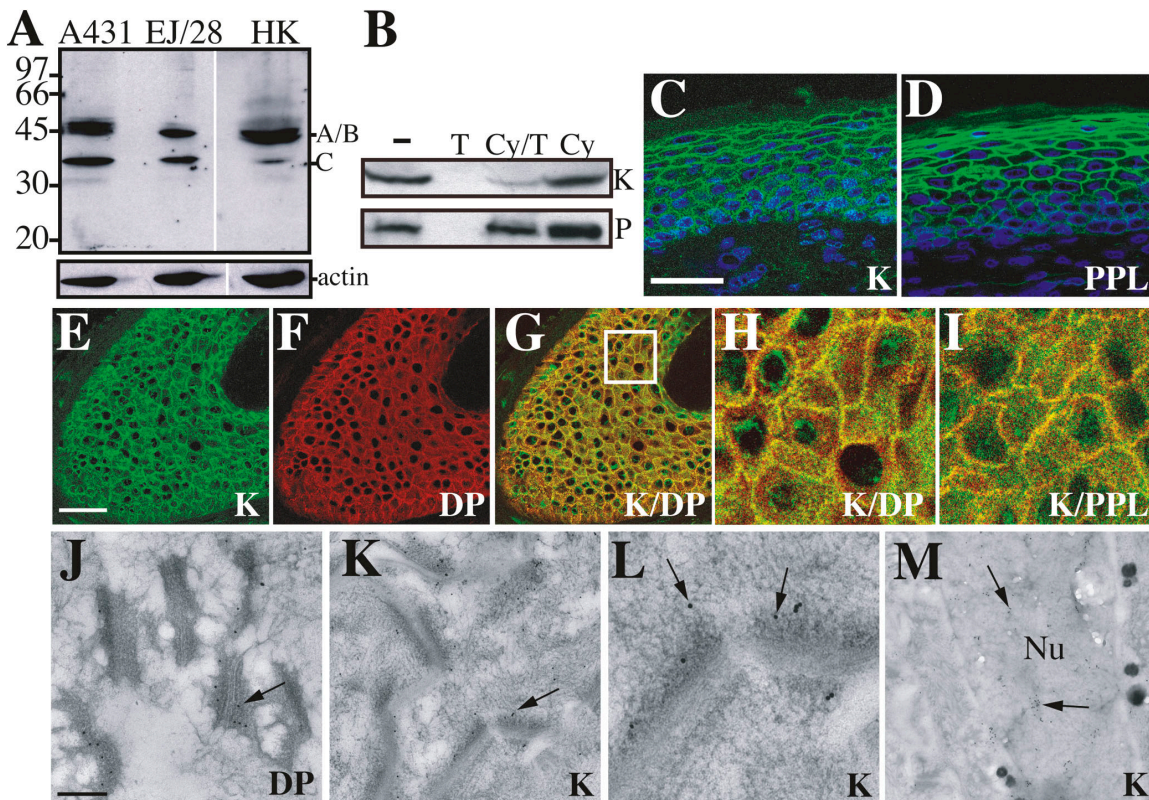


**Figure 4. Kazrin protein expression and cellular localization.** (A) Immunoblot of protein lysates from A431, EJ/28, and human keratinocytes (HK) with anti-kazrin (LS4) or anti-actin (loading control). The 37-kD band corresponds to kazrin C (C); the 47-kD doublet corresponds to kazrin A and B (A/B). Molecular mass markers (kD) are indicated. White line indicates that intervening lanes have been spliced out. (B) CE incorporation of periplakin and kazrin. Keratinocytes were incubated in the absence (–) or presence (T) of Triton X-100, cystamine (Cy), or cystamine and Triton X-100 (Cy/T). Immunoblots were probed with antibodies to kazrin (46 kD isoforms A/B are shown; K) and periplakin (P). (C–I) Immunofluorescence staining of human interfollicular epidermis (C and D) and hair follicles (E–I) with antibodies specific for kazrin (K; green in C, E, and G–I), periplakin (PPL; D, green; and I, red), or desmoplakin (DP; F–H, red). (C and D) Nuclei were labeled with TO-PRO-3 (blue). (G) Boxed area is enlarged in H. Bars: (C–G) 50  $\mu$ m; (H and I) 6  $\mu$ m. (J–M) Immunogold EM of human breast epidermis with anti-desmoplakin (J) and anti-kazrin (K–M). Arrows indicate 10-nm gold particles localized at desmosomes (J–L) or in nucleus (M). Bar: (J) 200 nm; (K) 330 nm; (L) 120 nm; (M) 487 nm.

interfollicular epidermis and in the hair follicle (Fig. 4, C and E). Periplakin was up-regulated in the suprabasal layers of the epidermis (Fig. 4 D). In the cell layers that coexpressed kazrin and periplakin, kazrin localized to cell–cell borders, but in the basal layer kazrin was more diffusely localized (Fig. 4, C and I). Double labeling for kazrin and periplakin or desmoplakin showed extensive colocalization at cell–cell borders (Fig. 4, E–I). In some cells, kazrin was detected in the nucleus (Fig. 4 H). Because both kazrin and periplakin (van den Heuvel et al., 2002) have a putative NLS it is possible that their interaction is not confined to the plasma membrane.

#### Kazrin is a desmosome component

Immunoelectron microscopy of human interfollicular epidermis confirmed that kazrin (Fig. 4, K and L), like desmoplakin (Fig. 4 J), was found at desmosomes. Some nuclei also showed kazrin labeling (Fig. 4 M). Whereas periplakin is found in association with keratin filaments (Ruhrberg et al., 1997), kazrin had a more diffuse cytoplasmic localization (not depicted).

In differentiating primary human keratinocytes, kazrin was observed at cell–cell borders and, to a variable degree, in

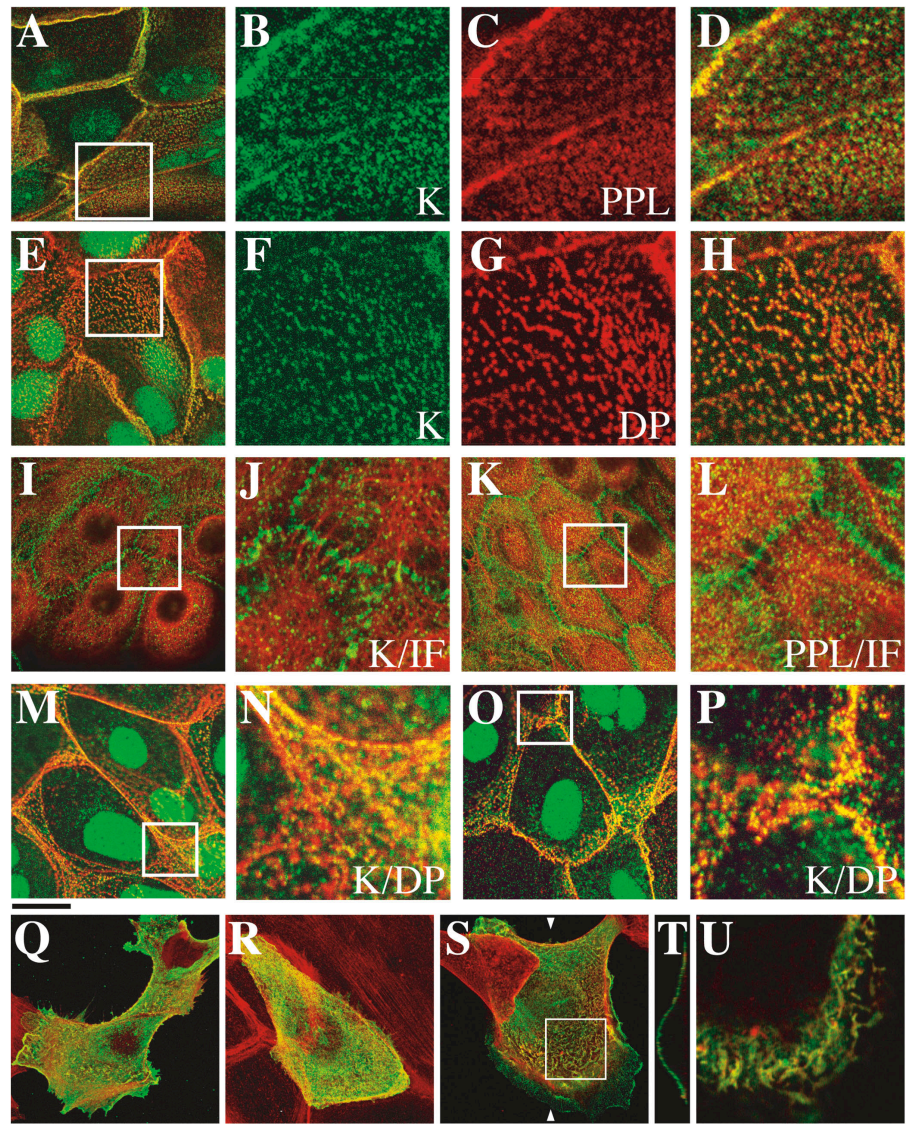
the nucleus (Fig. 5, A–L). In stratified cultures, large numbers of desmosomes assemble at the interface between the apical surfaces of basal layer cells and the basal surfaces of suprabasal cells. Kazrin partially colocalized with desmoplakin and periplakin at the desmosomes and with periplakin at the interdesmosomal plasma membrane (Fig. 5, A–H). Kazrin was localized to puncta, corresponding to desmosomes, where IFs in neighboring cells aligned (Fig. 5, I–L). The subcellular distribution of kazrin was indistinguishable in keratinocyte lines generated from periplakin-null and wild-type mice (Fig. 5, M–P), demonstrating that kazrin was not dependent on periplakin for its localization. The shift in kazrin localization to cell–cell borders in differentiating periplakin-null keratinocytes suggests an association with additional desmosomal components that are up-regulated during terminal differentiation.

#### Localization of kazrin protein isoforms

NH<sub>2</sub>-terminally HA-tagged constructs encoding kazrin A, B, or C were transiently transfected into primary human keratinocytes (Fig. 5, Q–U). All three isoforms had similar subcellular distributions (Fig. 5, Q–S) and were observed predominantly at the apical plasma membrane (Fig. 5, T and U), with



**Figure 5. Kazrin localization in cultured keratinocytes.** Human keratinocytes (A–L) and keratinocytes from wild-type (M and N) or periplakin null (O and P) mice were immunolabeled with antibodies to kazrin (K; A–J and M–P, green) and periplakin (PPL; A–D, red; and K and L, green), desmoplakin (DP; E–H and M–P, red) or keratins (IF; I–L, red). Boxes in A, E, I, K, M, and O are enlarged in B–D, F–H, J, L, N, and P, respectively. Bar: (A, E, I, K, M, and O) 20  $\mu\text{m}$ ; (B–D and F–H) 7  $\mu\text{m}$ ; (J and L) 5.4  $\mu\text{m}$ ; (N and P) 5  $\mu\text{m}$ . (Q–U) Kazrin isoforms (Q, kazrin A; R, kazrin B; S–U, kazrin C) with NH<sub>2</sub>-terminal HA tags were transiently transfected into primary human keratinocytes. (Q–U) green, anti-HA; red, phalloidin-TRITC. Q–S are composite images of z-stacks. Arrowheads in S indicate position of orthogonal view shown in T. Area boxed in S is shown as single confocal slice in U. Bar: (Q–S) 20  $\mu\text{m}$ ; (T) 11.5  $\mu\text{m}$ ; (U) 6  $\mu\text{m}$ .



some signal detected in the cytoplasm and the nucleus (not depicted). All isoforms could colocalize with cortical actin-based membrane structures including microvilli (Fig. 5, Q–U).

Although several proteins have been found to associate with the COOH terminus of periplakin (Aho and Kazerounian, 2003), kazrin is the first protein identified that binds to the NH<sub>2</sub> terminus. The association of periplakin and kazrin with actin and desmosomes, and the binding of periplakin to IFs, suggests that these proteins may be involved in the interplay between adherens junctions and desmosomes (Vasioukhin et al., 2001; Huen et al., 2002; Weber and Bement, 2002).

## Materials and methods

### Yeast two-hybrid screen and isolation of kazrin cDNA

Yeast two-hybrid protein interaction experiments and library screenings were performed using the MATCHMAKER GAL4 two-hybrid system 3 (BD Biosciences) according to the manufacturer's instructions. The AH109 yeast host strain was cotransformed with the bait plasmid (P133 in pGBKT7) and a human keratinocyte MATCHMAKER cDNA library in the cloning vector pGAD10.

### DNA clones and constructs

BLAST 2.0 (National Center for Biotechnology Information) and BLAT (Golden Path Genome Browser) programs were used to search EST databases and genome sequences. IMAGE clones of cDNAs encoding mouse periplakin (No. 349663), mouse kazrin a (No. 3667377), human kazrin a (No. 6180253), human kazrin b (No. 4556194), human kazrin c (No. 4651187), or human kazrin d (No. 4472821) were obtained from the Medical Research Council Geneservice Resource Centre and confirmed by sequencing the 5' UTRs and coding regions. See the online supplemental material for cloning strategies and PCR primer sequences.

### Cell culture and transfection

Normal neonatal human keratinocytes (strain kq passages 3–6) and spontaneously immortalized wild-type and periplakin-null (Aho et al., 2004) mouse keratinocytes were cultured as described previously (DiColandrea et al., 2000). All other cells were maintained in DME with 10% FCS. Transient transfection was performed as described previously (Karashima and Watt, 2002).

### Antibodies

The following primary antibodies were used as described previously (Ruhberg et al., 1997; Karashima and Watt, 2002): CR5 (rabbit anti-envoplakin), 11-5F (mouse monoclonal anti-desmoplakin; gift of D.R. Garrod, University of Manchester, Manchester, UK), TD2 (rabbit anti-periplakin), AC-40 (mouse monoclonal anti-actin; Sigma-Aldrich), AE11 (mouse monoclonal anti-periplakin; gift of H. Sun, New York University

Medical School, New York, NY), Y11 (rabbit antiserum to HA; Santa Cruz Biotechnology, Inc.), M2 (mouse monoclonal anti-FLAG; Sigma-Aldrich), and LP34 (mouse monoclonal anti-keratin). Alexa 488- or Alexa 594-conjugated secondary antibodies (Molecular Probes) were used.

A peptide corresponding to the predicted COOH-terminal 20 amino acids (DPGLFDGTAPDYIEEDADW) of human and mouse kazrin was used to generate rabbit anti-LS4. LS4 was affinity purified on a column containing its immunogen coupled to Amino-Link Coupling Gel (Perbio).

### GST pull down assay

Fusion proteins were expressed in *Escherichia coli* BL21 cells and purified from cell extracts using Glutathione Sepharose 4B (Amersham Biosciences). Confluent cultures of human keratinocytes were extracted in ice-cold buffer (50 mM NaCl, 300 mM sucrose, 10 mM Pipes, pH 6.8, 3 mM MgCl<sub>2</sub>, and 0.5% Triton X-100) containing 10 mM EDTA and protease inhibitors (Roche). Protein samples were incubated by rotation at 4°C for 3–4 h with 10 µg GST or GST-fusion proteins prebound to Glutathione Sepharose 4B. Precipitates were washed in ice-cold PBS and boiled in SDS-PAGE sample buffer containing 10% β-mercaptoethanol before gel electrophoresis.

### Immunodetection

Immunofluorescence staining was performed as described previously (DiColandrea et al., 2000). Samples were examined on a laser scanning confocal microscope (model LSM 510 equipped with 458-nm, 488-nm, and 633-nm lasers; Carl Zeiss MicroImaging, Inc.) with a 63× plan-APO-CHROMAT oil immersion lens (numerical aperture 1.4) or 40× C-APO-CHROMAT water immersion lens (numerical aperture 1.2). Digital images were prepared using Adobe Photoshop 6.0 and Imaris 3.1. Immunogold electron microscopy was performed on thin sections of high pressure-frozen and freeze-substituted adult breast epidermis (Ruhrberg et al., 1996). Immunoprecipitation and immunoblotting were performed as described previously (Ruhrberg et al., 1996).

### In situ hybridization and RT-PCR

In situ hybridization was performed with sections of PFA-fixed, paraffin-embedded mouse tissues and <sup>35</sup>S-labeled riboprobes described in the online supplemental material.

Total RNA was prepared from cultured cells using TriReagent (Molecular Research Center, Inc.). The SuperScript One-Step RT-PCR with Platinum Taq kit (Invitrogen) was used to determine expression of human kazrin mRNA in a panel of primary cells and cell lines. Details of primer sequences can be found in the online supplemental material.

### Online supplemental material

Fig. S1 shows kazrin nucleotide and amino acid sequences. Fig. S2 shows analysis of predicted structure and hydrophilicity of kazrin. Fig. S3 shows real-time PCR analysis of kazrin expression. Online supplemental material is available at <http://www.jcb.org/cgi/content/full/jcb.200312123/DC1>.

We thank Mike Mitchell for assistance with database searches and Peter Jordan and Daniel Zicha for advice on confocal microscopy. We thank Michaela Frye, Josema Torres-Ibañez, and Laura Turner for help with experiments. We are most grateful to the Cancer Research UK In Situ Hybrid-

isation service and the Electron Microscopy service.

This work was supported by Cancer Research UK. L.M. Sevilla was supported by a National Institutes of Health fellowship (HD42379-02).

Submitted: 17 December 2003

Accepted: 23 July 2004

## References

- Aho, S., and S. Kazerounian. 2003. Molecular interactions of periplakin in epithelial cells. *Recent Res. Dev. Cell Biochem.* 1:133–141.
- Aho, S., L. Kehua, R. Young, C. McGee, A. Ishida-Yamamoto, J. Uitto, and J. Klement. 2004. Periplakin gene targeting reveals a constituent of the cornified cell envelope dispensable for normal mouse development. *Mol. Cell. Biol.* 24:6410–6418.
- Bretscher, A., K. Edwards, and R.G. Fehon. 2002. ERM proteins and merlin: integrators at the cell cortex. *Nat. Rev. Mol. Cell Biol.* 3:586–599.
- DiColandrea, T., T. Karashima, A. Määttä, and F.M. Watt. 2000. Subcellular distribution of envoplakin and periplakin: insights into their role as precursors of the epidermal cornified envelope. *J. Cell Biol.* 151:573–586.
- Fuchs, E., and I. Karakesisoglou. 2001. Bridging cytoskeletal interactions. *Genes Dev.* 15:1–14.
- Huen, A.C., J.K. Park, L.M. Godsel, X. Chen, L.J. Bannon, E.V. Amargo, T.Y. Hudson, A.K. Mongiu, I.M. Leigh, D.P. Kelsell, et al. 2002. Intermediate filament–membrane attachments function synergistically with actin-dependent contacts to regulate intercellular adhesive strength. *J. Cell Biol.* 159:1005–1017.
- Kalinin, A., L.N. Marekov, and P.M. Steinert. 2001. Assembly of the epidermal cornified cell envelope. *J. Cell Sci.* 114:3069–3070.
- Kalinin, A.E., A.V. Kajava, and P.M. Steinert. 2002. Epithelial barrier function: assembly and structural features of the cornified cell envelope. *Bioessays.* 24:789–800.
- Karashima, T., and F.M. Watt. 2002. Interaction of periplakin and envoplakin with intermediate filaments. *J. Cell Sci.* 115:5027–5037.
- Leung, C.L., K.J. Green, and R.K. Liem. 2002. Plakins: a family of versatile cytolinker proteins. *Trends Cell Biol.* 12:37–45.
- Ruhrberg, C., M.A. Hajibagheri, M. Simon, T.P. Dooley, and F.M. Watt. 1996. Envoplakin, a novel precursor of the cornified envelope that has homology to desmoplakin. *J. Cell Biol.* 134:715–729.
- Ruhrberg, C., M.A. Hajibagheri, D.A. Parry, and F.M. Watt. 1997. Periplakin, a novel component of cornified envelopes and desmosomes that belongs to the plakin family and forms complexes with envoplakin. *J. Cell Biol.* 139:1835–1849.
- van den Heuvel, A.P., A.M. de Vries-Smits, P.C. van Weeren, P.F. Dijkers, K.M. de Bruyn, J.A. Riedl, and B.M. Burgering. 2002. Binding of protein kinase B to the plakin family member periplakin. *J. Cell Sci.* 115:3957–3966.
- Vasioukhin, V., E. Bowers, C. Bauer, L. Degenstein, and E. Fuchs. 2001. Desmoplakin is essential in epidermal sheet formation. *Nat. Cell Biol.* 3:1076–1085.
- Weber, K.L., and W.M. Bement. 2002. F-actin serves as a template for cyokeratin organization in cell free extracts. *J. Cell Sci.* 115:1373–1382.